FLEX End-to-End Mission Performance Simulator

Jorge Vicent, Neus Sabater, Carolina Tenjo, Juan Ramón Acarreta, María Manzano, Juan Pablo Rivera, Pedro Jurado, Raffaella Franco, Luis Alonso, Jochem Verrelst, and José Moreno, *Member, IEEE*

***Abstract*—The FLuorescence EXplorer (FLEX) mission, selected as the European Space Agency's eighth Earth Explorer, aims to globally measure the sun-induced-chlorophyll-fluorescence spectral emission from terrestrial vegetation. In the frame of the FLEX mission, several industrial and scientific studies have analyzed the instrument design, image processing algorithms, or modeling aspects. At the same time, a common tool is needed to address the overall FLEX mission performance by combining all these features. For this reason, an end-to-end mission performance simulator has been developed for the FLEX mission (FLEX-E). This paper describes the FLEX-E software design, which combines the generation of complex synthetic scenes with an advanced modeling of the instrument behavior and the full processing scheme up to the final fluorescence product. The results derived from FLEX-E simulations indicate that the instrument and developed image processing algorithms are able to retrieve the sun-induced fluorescence with an accuracy below the 0.2 $\mathbf{mW \cdot m^{-2} \cdot sr^{-1} \cdot nm^{-1}}$ mission requirement. It is expected that FLEX-E will not only optimize the FLEX retrieval algorithms and technical requirements, but also serve as the baseline for the ground processing implementation and testing of calibration/ validation procedures.**

***Index Terms*—FLuorescence EXplorer (FLEX), hyperspectral, imaging spectrometer, mission simulator, radiative transfer, Sentinel-3 (S3), sun-induced chlorophyll fluorescence (SIF), tandem, validation.**

I. Introduction

THE performance of the European Space Agency's (ESA) FLuorescence EXplorer (FLEX) mission [1] has been analyzed in several interdependent industrial and scientific studies. Projects such as PARCS [2] and Phytosynthesis Study [3] have consolidated the FLEX mission requirements, developed a sun-induced chlorophyll fluorescence (SIF) retrieval algorithm, and investigated the linkage between SIF and photosynthesis. The industrial studies have analyzed and developed the engineering issues of the FLEX platform and instrument. While these studies helped to consolidate the mission specifications, the competitive ESA mission selection process is largely based on an analysis of the results as produced by an end-to-end mission performance simulator (E2ES). The E2ES must combine all the different mission aspects and be designed following the guidelines in [4] and [5]. For this reason, a FLEX E2ES (called FLEX-E) has been developed in order to test the accuracy of the retrieved SIF and overall mission performance.

As part of satellite mission development, E2ESs have been studied, developed, and applied for the last two decades [6]–[12]. These software tools reproduce all aspects of satellite missions, including the platform orbit/attitude, synthetic scene radiative transfer generation, sensor behavior, ground image processing, and product evaluation. E2ESs are unique frameworks to determine the mission characteristics impacting the data quality and achievement of scientific goals, enabling the consolidation of the mission requirements and checking the consistency of platform and payload specifications. These tools support tradeoff studies and are useful in the preparation for system calibration tests. From an image processing perspective, E2ESs allow testing and optimizing the retrieval schemes prior to the mission operations [13], [14].

The objectives of this paper are twofold: 1) to present the FLEX-E and 2) to demonstrate its suitability to assess the performance of the mission concept and implemented processing algorithms. By using FLEX-E, this paper will demonstrate that the FLEX mission fulfills the mission requirements by retrieving SIF below the 0.2 $\mathrm{mW \cdot m^{-2} \cdot sr^{-1} \cdot nm^{-1}}$ threshold. The versatility of FLEX-E allows to generate simulated images for three instruments through a realistic radiative transfer and instrument modeling.

This paper is structured as follows. An overview of the FLEX mission is given in Section II, followed by a brief description of the FLEX-E design (see Section III). By using FLEX-E over a test scenario, the potential of the FLEX mission concept and developed SIF retrieval algorithms are demonstrated in Section IV. This paper concludes with an outlook of how the FLEX-E too will evolve in future phases of the mission.

II. Overview of the FLEX/S3 Tandem Mission

The FLEX mission has been specifically designed and optimized to globally measure SIF spectral emission from terrestrial vegetation [15]. The SIF spectrum (see Fig. 1), characterized by two peaks (with maxima at approximately 685 and 740 nm) and its total spectrally integrated energy, is a sensitive indicator of the actual photosynthetic activity in vegetation. SIF can

Manuscript received November 2, 2015; revised January 28, 2016; accepted March 1, 2016. This work was supported by the European Space Agency under the ESA-ESTEC Contract 4000108364/13/NL/BJ.

J. Vicent, N. Sabater, C. Tenjo, J. P. Rivera, J. Verrelst, and J. Moreno are with the Image Processing Laboratory, University of Valencia, 46980 Valencia, Spain (e-mail: jorge.vicent@uv.es; m.neus.sabater@uv.es; nancy.tenjo@uv.es; juan.rivera@uv.es; jochem.verrelst@uv.es; jose.moreno@uv.es).

J. R. Acarreta is with Deimos Space S.L.U., 28760 Madrid, Spain (e-mail: juan-ramon.acarreta@deimos-space.com).

M. Manzano is with GMV Aerospace and Defence Space S.A.U., 28760 Madrid, Spain (e-mail: mmanzano@gmv.com).

P. Jurado and R. Franco are with the European Space Research and Technology Centre (ESTEC), European Space Agency, 2201 AZ Noordwijk, The Netherlands (e-mail: pedro.jurado@esa.int; raffaella.franco@esa.int).

L. Alonso is with the Image Processing Laboratory, University of Valencia, 46010 Valencia, Spain, and also with Institute of Biometeorology (IBIMET)-CNR, 50145 Firenze, Italia (e-mail: luis.alonso@uv.es).

Color versions of one or more of the figures in this paper are available online at http://ieeexplore.ieee.org.

Digital Object Identifier 10.1109/TGRS.2016.2538300

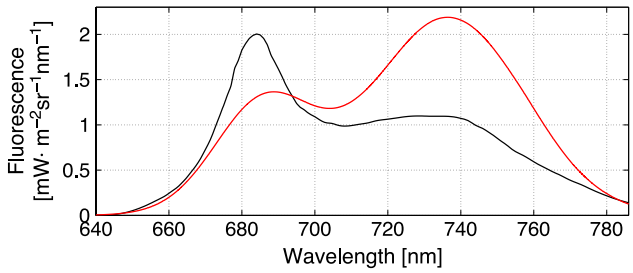

Fig. 1. Example of two SIF spectra for different species and/or stress conditions.

be used as a powerful noninvasive marker to track the status, resilience, and recovery of photochemical processes [16]. Determining this SIF emission is of particular interest for the refined predictive capability of global carbon cycle models through improved parameterizations of canopy photosynthetic activity and surface-atmosphere water and energy exchange processes [17], [18].

The FLEX mission consists of a single platform with two imaging pushbroom spectrometers (FLORIS-HR and FLORIS-LR) [19] acquiring in the 500–780-nm spectral range at high (0.3 nm) and low (2 nm) spectral resolutions, respectively. FLEX will fly in tandem with Copernicus' Sentinel-3 (S3) satellite [20], acquiring data over the same target with 6–15-s time delay at 300-m spatial sampling and 150-km swath. The synergy between FLORIS and S3 OLCI and SLSTR Level-1b data enables to characterize the atmospheric state and to determine key vegetation biophysical parameters for a reliable retrieval of the SIF. Given the need to reproduce the tandem flight, the FLORIS high spectral resolution and the validation of the retrieved SIF are explicitly taken into account in the design and implementation of FLEX-E. The FLEX/S3 mission key sensor characteristics are summarized in Table I.

TABLE I
FLORIS, OLCI, AND SLSTR SENSOR CHARACTERISTICS AS PER [1] AND [21]

	FLORIS-HR	FLORIS-LR
Imaging principle	Pushbroom-grating	
# pixels×bands	∼500×292	∼500×245
Spectral range [nm]	677–697 (O_2-B) 740–780 (O_2-A)	500–780
Spectral resolution	0.3 nm	2 nm
Spectral sampling	0.1 nm	0.7 nm
Spectral coregistration	0.01 nm	
Swath width	150 km	
Spatial sampling	300 m	
Spatial coregistration	45–90 m	
Geolocation accuracy	120 m	
SNR @L_{ref}	115–1015 (See Fig. 7)	
Radiometric accuracy	5% abs, 1% rel	
Radiometric resolution	16 bit	
Coverage	Land, coastal areas, major islands	
Revisit time	<27 days	

	OLCI	SLSTR
Imaging principle	Pushbroom grating	Scanning radiometer
# bands	21	9
Spectral range [nm]	400–1020	555–12000
Spectral resolution	2.5–40 nm	20–1000 nm
Swath width [km]	1270	1420 (nadir) 740 (oblique)
Spatial sampling	0.3 km	0.5–1 km
SNR @L_{ref}	150–2200	25–900
NeΔT	n.a.	20–80 mK (TIR)
Radiometric accuracy	2% abs, 1% rel	2% (VIS-SWIR) 0.1 K (TIR)
Radiometric resolution	14 bit	
Coverage	Global	
Revisit time	<2.2 days	<1.8 days

III. FLEX-E Architecture Design

The FLEX-E design is based on the guidelines outlined in [4] where an entire remote-sensing system is divided into multiple parts, so-called *high-level modules* (see Fig. 2). These modules encompass different areas of the platform, instrument, and signal modeling and are integrated and streamlined within a simulator framework such as openSF [5]. Following these guidelines for designing an E2ES does enable the comparative analysis of the results produced by other competitive mission simulators (e.g., ESA open calls for Earth Explorer).

A. Geometry Modules

The geometry modules are in charge of simulating the satellite orbit and attitude, as well as the generation of the observation geometry of each instrument. They are constrained by the FLEX/S3 tandem flight configuration. This implies that each sensor, given the specific illumination and observation geometry, acquires different radiances from the same target area. The usage of the full 3-D geometry along the processing chain guarantees the consistent geometrical treatment when projecting each instrument focal plane on ground and the explicit accounting for all topographic effects. For this reason, the FLEX and S3 geometry modules are run in the first place following the approach in [8]. Accounting for the illumination and observation geometry in the forward modeling of the scene generation offers an advantage with respect to conventional E2ES where the scene is generated prior and independently of the observation geometry (e.g., [6] and [11]).

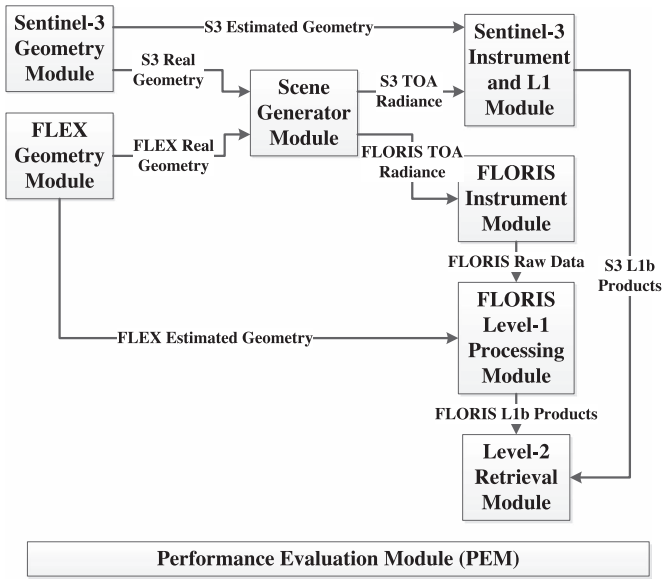

Fig. 2. FLEX-E high-level modular architecture and data flow. For clarity, the links between all the modules and the PEM have been omitted.

After the user selection of the geographical coordinates of the ground target area and the acquisition epoch, the geometry modules calculate the real geometry through the orbit segment and line of sight (LOS) for each acquisition time and pixel in the satellite focal plane [22]. The tandem configuration is ensured by the use of FLEX and S3 full orbit cycles with a configurable time delay between them. Based on the orbit cycles, each module calculates the orbit segment when the satellite overpass the target area closest to the nadir observation and selected acquisition time. The LOS is calculated taking the instrument scanning motion as well as the instrument mounting, the platform attitude, and all the geometrical distortions and colocation issues into account. Both geometry modules also calculate the estimated geometry, including the platform orbit/attitude and instrument mounting errors, necessary for the simulation of the Level-1b geolocation.

B. SGM

The scene generator module (SGM) [23] propagates solar radiation through the canopy and atmosphere, simulating on a pixel-by-pixel basis the target scenes for FLEX and S3 sensors. The scenes are defined according to key biophysical, atmospheric, and topographic input parameters and consist of high-spectral-resolution top-of-atmosphere (TOA) radiance spectra L_{scn} distributed over a high spatial resolution grid. Their resolution is at least an order of magnitude finer than the instrument resolution in order to simulate the instrument acquisition through its spatial/spectral response functions. A common scene grid is set for the FLEX and S3 instruments, which enables the SGM to generate intrinsically different but consistent scenes for each sensor. This is possible by considering the specific instrument observation geometry and spectral configuration while keeping the same definition of the canopy, atmosphere, and topographic properties. The SGM is subdivided into three blocks.

- The *scene definition* block distributes key biophysical and atmospheric input parameters (e.g., leaf area index (LAI), chlorophyll content, and aerosol type/content) over the scene grid. This is achieved based on global or user-defined land cover class maps [24], atmospheric data [25], and surface topography [26]. Each land cover class is associated with a database that defines the surface reflectance or, alternatively, the range and statistical/spatial distribution of the key biophysical parameters to be input in a radiative transfer model (RTM).
- The *geometry-scene interaction* block determines the viewing and illumination conditions over each scene grid point, considering the surface topography, platform orbit position, and sensor LOS at each acquisition time [27]. In order to properly convolve the reference high-resolution scene with an accurate instrument response function that accounts for technical aspects in the optics and detectors, the instrument module requires the focal plane coordinates corresponding to each surface grid point. This is achieved by the *geometry-scene interaction* block, firstly projecting the sensor pixel center onto the 3-D surface (using DEM) and secondly resampling these pixel coordinates for each scene grid point.
- The *forward model* block must simulate TOA radiance spectra, including SIF, at very high spectral resolution. Accordingly, the SGM relies on two RTMs. At the canopy scale, the SCOPE model [28] is implemented in the SGM due to its capability to simulate surface bidirectional reflectance and SIF. These simulations are then coupled with the atmospheric MODTRAN5 model [29], which is used for the simulation of atmospheric effects to properly account for narrow atmospheric absorption bands. These models use biophysical and atmospheric input parameters, together with the observation/illumination geometry and surface topography, to propagate the light through the canopy and atmosphere. Thus, the *forward model* block generates, according to Verhoef and Bach [30] and Guanter *et al.* [31], the surface reflectance, SIF, and TOA radiance spectra that are also used as reference for the evaluation of the Level-1b and Level-2 products.

The use of land cover class maps and atmospheric data in combination with the running of RTMs offers important advantages as opposed to the use of external reflectance maps or airborne images [32]. First, the RTM-generated scenes are noise free, whereas the use of external images introduces their instrumental characteristics (e.g., noise and calibration). Second, the RTM-generated scenes are unconstrained by the observation/illumination geometry of the external images. Finally, the scene definition according to key biophysical and atmospheric parameters allows to evaluate the quality of the Level-2 retrieval algorithms in a wider range of cases. Moreover, the spectral and/or spatial resolution of currently available airborne/spaceborne imaging spectrometers are insufficient for the simulation of the very high spectral resolution scenes required for FLEX [33].

In order to evaluate the accuracy of the Level-1b and Level-2 products, the SGM resamples the high-resolution data to the instrument resolution for a pixel-to-pixel comparison against the instrument output. This resampling is achieved by the convolution of the high-resolution data with the instrument spatial and spectral response functions based on the input instrument LOS and spectral configuration.

C. Instrument and Level-1 Processing Modules

Two parallel chains of instrument and Level-1 processing modules are executed to simulate the scene signal acquisition by FLEX and S3. Regarding FLEX, the simulation of the FLORIS instrument and its Level-1b processing is carried out in two independent modules: 1) the FLORIS instrument module and 2) the FLORIS Level-1 processing module. These two modules implement a detailed representation of the actual instrument design and data processing [1]. The FLORIS instrument module simulates the FLORIS spatial–spectral behavior by resampling the high-resolution scene to the lower instrument resolution for each spectral band λ_{sen} and instrument focal plane pixel coordinates (l, c) according to

$$L_{\mathrm{sen}} = \int\int\int F_{\mathrm{psf}}(\lambda_{\mathrm{sen}}, c) \cdot F_t(l) \cdot L_{\mathrm{scn}} \cdot dxdyd\lambda_{\mathrm{scn}}. \quad (1)$$

With F_{psf} being the instrument response function due to the optics and F_t being the effect of the integration time

along track. These functions are modeled through the effects of telescope diffraction, optical aberration, slit width in the along-track direction, smearing length, pixel size at detector level in the across-track direction (including binning), pixel spectral extent, along-track line spread function, and uniformity of the detectors. In addition, the spatial and spectral stability effects such as keystone and spectral smile are included in order to model the acquisition for each line and column. The instrument module generates noise-free equivalent Level-1b radiance data $L_{\text{sen}}(\lambda_{\text{sen}}; l, c)$ used to analyze the radiometric noises and calibrations errors. The L_{sen} is modified by the stray-light (L_s) contribution according to

$$L'_{\text{sen}} = L_{\text{sen}} + L_s(L_{\text{sen}}; c, l, \lambda_{\text{sen}}). \quad (2)$$

L_s is obtained by applying a spatial–spectral kernel on L_{sen} at each acquisition line. This kernel includes the effects of the optical surface roughness/contamination, focal plane filter, grating dispersion, and focal length of the telescope. The resampled signal L'_{sen} is then passed to the FLORIS acquisition chain, simulating all the sensor electronics and onboard processing. This produces at-sensor raw data in digital counts with the following features:

- spectral/spatial radiometric random and systematic noises, i.e., vertical pattern, dark current, temporal noise, photonic noise, readout, and smearing;
- detector and video-chain noises, including the analog-to-digital conversion;
- spatial and temporal coregistration between each FLORIS spectrometer and within each spectrometer.

The FLORIS Level-1 processing module recovers the radiance level from the raw data by applying the dark signal and absolute/relative estimated calibration coefficients, thus including the propagation of radiometric calibration errors. Spectral calibration errors are included through spectral shift and bandwidth stretch in the real central wavelengths λ_{sen}. The Level-1 processing module also corrects the nonuniformities in the detector caused by defectuous pixels or anomalies in the sensor [34]. The geolocation assigns the latitude/longitude coordinates to each pixel from the estimated platform orbit/attitude and the FLORIS mounting within the platform.

Regarding S3, an equivalent chain generating OLCI and SLSTR Level-1b data has been developed within the S3 instrument and Level-1 module. Given that S3 is an external mission, no performance tests on S3 instruments are carried out in FLEX-E. Therefore, the simulation of the instrument noises and their correction at Level-1 is simplified by considering a random noise realization based on the nominal signal-to-noise ratio (SNR) [21]. The custom-made S3 module includes all the relevant instrumental and platform characteristics and allows to develop FLEX-E unconstrained by ESA's S3 E2ES yet with a representative simulation of the S3 instruments and their Level-1b processing.

D. Level-2 Retrieval Module

The Level-2 retrieval module is designed in a way that it accounts for all atmospheric and surface effects included in the forward scene simulation and the realism of the instrument and Level-1 processing modeling. The implemented Level-2 retrieval module aims to reproduce the ground processing with such a level of detail so that it can be reused with real FLEX and S3 data and serve as basis for its future implementation. The synergy between FLORIS, OLCI, and SLSTR Level-1b products is achieved by running the following sequence of image processing algorithms.

1) The FLEX and S3 Level-1b products are *geometrically coregistered* into a common spatial grid in order to exploit their data in synergy. The coregistration uses the Level-1b geolocation coordinates without ground control points and makes a bidimensional cubic spline interpolation of OLCI, SLSTR, and FLORIS-LR into the FLORIS-HR grid.
2) The *spectral recalibration* of the FLORIS-HR Level-1b data reduces the residual errors from the onboard calibration. The implemented spectral recalibration is a refined version of the O_2 absorption feature matching algorithm in [35]. It approximates the instrument response by a double error function for which the central wavelength, bandwidth, and shape parameters are tuned [36].
3) The *radiometric cross-calibration* of the coregistered FLORIS and OLCI Level-1b data enables having consistent radiance measurements and corrects for the residual radiometric calibration errors in FLORIS data. The cross-calibration simulates synthetic OLCI bands within the 500–800-nm range, excluding atmospheric absorption features, by the convolution of the FLORIS spectrum with the OLCI spectral response function. The ratio between the synthetic and real OLCI bands is linearly interpolated to the full FLORIS spectral range.
4) The *atmospheric correction* scheme retrieves the aerosol properties and water vapor through a lookup table inversion method using the coregistered S3 Level-1b data (see [1], [37], and [38] for more details). The atmospherically corrected data (i.e., surface apparent reflectance and solar irradiance) are obtained from the inverse MODTRAN5 radiative transfer modeling based on the characterized atmospheric parameters. The atmospheric correction scheme includes a cloud-screening algorithm and obtains the surface temperature using the SLSTR thermal channels.
5) The FLORIS spectral range and resolution are suitable for the application of spectral fitting methods (SFMs) for *SIF retrieval*. SFM proved to be robust under noisy instrument data [15]. From FLORIS atmospherically corrected data, SFM decouples the surface reflectance and SIF within the O_2 absorption bands and reconstructs the full SIF emission spectrum (see Fig. 3). An advanced SFM has been implemented and optimized for the FLORIS configuration [39]. Additionally, FLORIS and S3 data are used in synergy to retrieve additional key biophysical parameters (e.g., LAI and chlorophyll content) [40].

E. PEM

The performance evaluation module (PEM) is a plotting and reporting tool that evaluates the mission performance through the comparison of the Level-1b and Level-2 products against their reference data from the geometry, SGM, and instrument

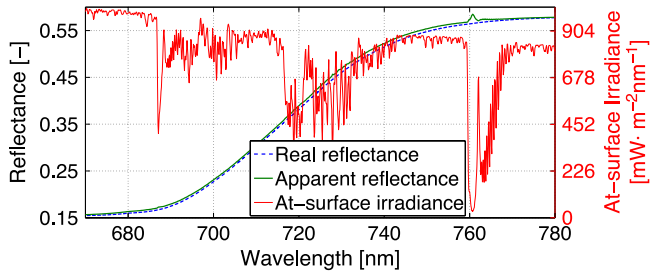

Fig. 3. O_2 absorption bands allow decoupling the SIF emission from the (blue) real reflectance based on the peaks in the (green) apparent reflectance.

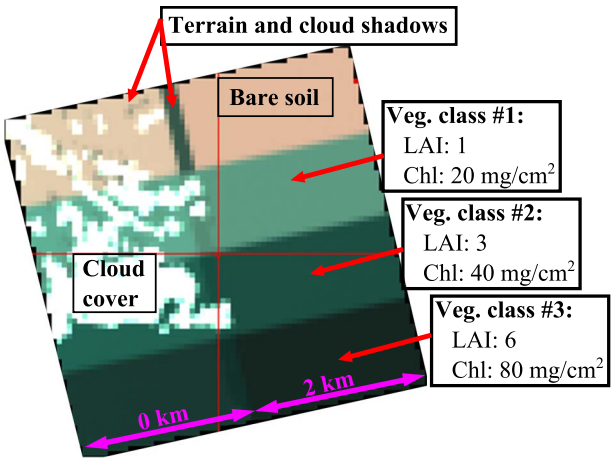

Fig. 4. RGB composite of the test scenario Level-1b image.

modules. This module is executed at the end of the simulation chain, and it is fully independent from the modules described in the previous paragraphs. The PEM aims to accomplish the following:

- verify that the SIF and key biophysical parameters are correctly retrieved;
- check the accuracy of the retrieved atmospheric parameters and inverted surface reflectance;
- analyze the performance of the geolocation algorithms and errors in the estimated observation geometry;
- study the recovery of pixel uniformity and radiometric/spectral calibration in the Level-1b products;
- assess the impact of the instrumental noises on the Level-1b and Level-2 products.

For this purpose, the PEM includes these capabilities:

1) the computation of band-per-band error maps and spectrum pixelwise error metrics;
2) Monte Carlo statistical analysis for each data set;
3) generation of spectral plots and images.

IV. Results and Discussion

In order to evaluate the performance of the FLEX mission to retrieve SIF below a 0.2 mW · m^{-2} · sr^{-1} · nm^{-1} error, FLEX-E has been executed on a 20 km × 20 km test scenario (see Fig. 4). Despite the FLEX-E capability to generate complex and realistic scenes, the simulation of a scene made of simple geometric patterns facilitates the evaluation of the mission performance. This scenario is made of four homogeneous land cover classes, being a nonfluorescent target (bare soil), and three vegetation

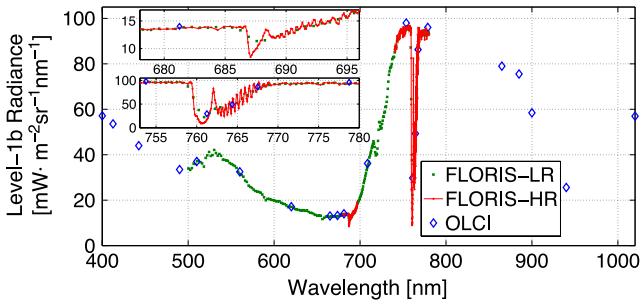

Fig. 5. Sample Level-1b radiance spectra for (green) FLORIS-LR, (red) FLORIS-HR, and (blue) OLCI.

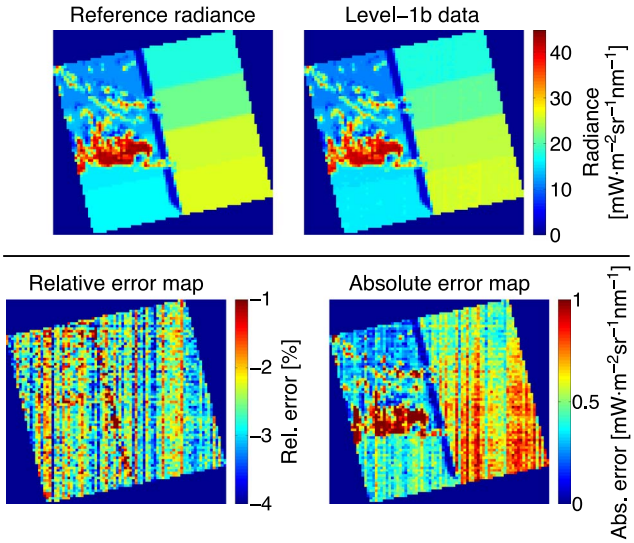

Fig. 6. FLORIS-HR Level-1b performance within the O_2-A absorption band. (Top left) Reference radiances after convolution of the scene with the ideal instrument response. (Top right) Level-1b data after recalibration of the raw data. (Bottom left/right) Relative and absolute error maps between reference and Level-1b radiance.

classes ranging from low to high SIF. The digital elevation model consists of two vertical stripes of 10 km × 20 km at an altitude of 0 and 2 km, respectively. A cumulus cloud cover is included in the scenario in order to analyze the effect of instrument stray light in the mission products. Shadows caused by the terrain topography and cloud cover are also calculated according to the illumination geometry. The atmosphere is defined as the standard midlatitude summer type with a continental aerosol load of 0.15 optical thickness. The scene is observed with a mean observation zenith angle of 1° and a mean solar zenith angle of 43°.

The end-to-end simulation includes all the instrumental noises, nonuniformity effects, and Level-1b calibration errors such as stray light, spectral stability, spectral/spatial radiometric noises, detector and video-chain noises, spatial/spectral/temporal coregistration errors, geolocation errors, and spectral/radiometric calibration errors, as described in Section III. Fig. 5 shows a sample FLORIS and OLCI Level-1b TOA radiance spectrum from the vegetation class #2.

The quality assessment of the retrieved SIF needs the prior validation of the Level-1b products against the mission requirements [41]. The simulated Level-1b radiometric performance is exemplified in Fig. 6 for the FLORIS-HR spectrometer at the

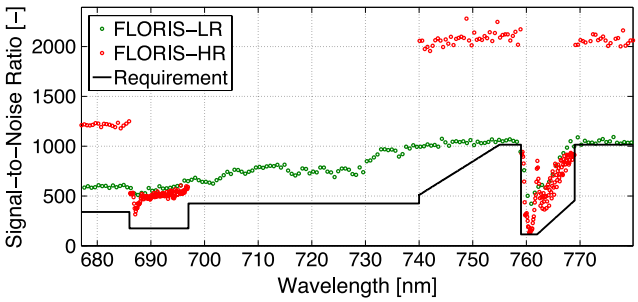

Fig. 7. SNR for the (green) FLORIS-LR and (red) FLORIS-HR spectrometers compared with the (black line) mission requirements.

TABLE II
LEVEL-1B MISSION REQUIREMENTS AND ACHIEVED PERFORMANCE BASED ON FLEX-E RESULTS

Mission Requirement	Results
Geometric performance:	
• Geolocation accuracy (120 m)	90 ± 4 m
• Sampling distance (300 m)	301 ± 1 m
Spectral performance (FLORIS-HR):	
• Resolution (0.3 nm)	0.3 nm
• Sampling interval (0.1 nm)	0.1 nm
• Smile (0.01 nm)	<0.01 m
• Calibration error (0.325 nm)	<0.08 nm
Radiometric performance:	
• Absolute calibration (5%)	$2.2 \pm 0.2\%$
• Relative calibration (1%)	$0.93 \pm 0.02\%$

O_2-A spectral channel. The accompanied relative and absolute error maps show the effects of the noises implemented in the simulator, composed by random contributions (modeled by using Monte Carlo methods) and scene-level systematic effects such as stray light, smile, and heterogeneity effects in individual detector pixels. The absolute error maps show higher instrument noises at higher radiance levels, particularly for the bright cloud pixels and for the 2-km altitude (with less atmospheric absorption), particularly for denser vegetation (i.e., vegetation class #2 and #3 that have higher near-infrared reflectance).

The implemented instrument noises and errors reproduce the expected error level and spatial pattern for real FLEX images. Indeed, the SNR derived from the Level-1b data over a homogeneous scene of an average vegetation radiance spectrum [41] matches the mission requirement (see Fig. 7).

The additional validation of the Level-1b products at geometric, spectral, and radiometric levels is summarized in Table II (see [1] for details).

The generated results lead to the following observations.

- The Level-1b geolocation satisfies the mission requirements with the expected knowledge of the FLORIS mounting Euler angles and attitude/orbit errors, even without the use of ground control points.
- The spectral sampling/resolution requirements are met by matching the optical performance (e.g., spot size and magnification), grating dispersion, and detector pixel size.
- The smile effect shows a parabolic behavior symmetric with respect to the swath center. The performance requirement is met both in the binned and not-binned channels.
- The spectral calibration varies linearly with the spectral channel, being, in any case, within the requirement.

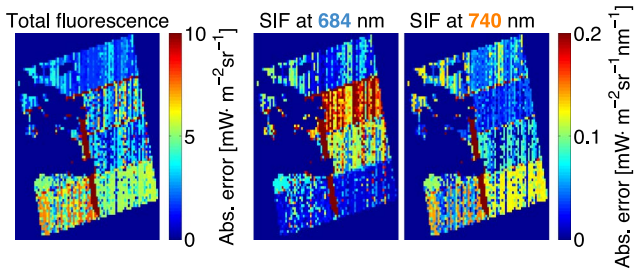

Fig. 8. Absolute error maps for the (left) Level-2 retrieved total SIF and peak values at (middle) 684 nm and (right) 740 nm. Clouds are masked in the retrieval process.

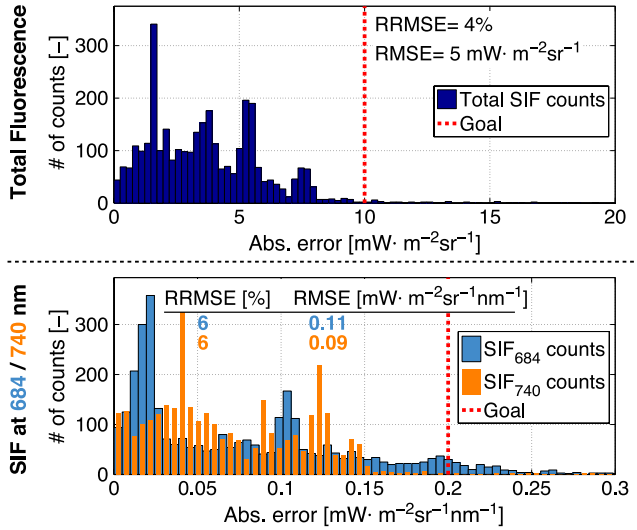

Fig. 9. Absolute error histogram for the (top) Level-2 retrieved total SIF and (bottom) peak values at 684 nm and 740 nm.

- The absolute and relative radiometric calibration is within the requirements, considering all the instrument noises, nonuniformity effects, and calibration errors.

The achieved mission performance for the Level-2 products is evaluated based on the absolute error map defined as the difference between the reference and retrieved SIF (see Fig. 8). The highest errors are found at O_2-B for vegetation class #1 and at O_2-A for vegetation class #3. Both cases correspond to the highest proportion of reflected radiance with respect to the SIF of all vegetation classes. In particular, in the case of O_2-B and low vegetation (LAI $= 1$), there is a larger contribution of the background soil, which increases the reflected red signal together with a smaller chlorophyll absorption, resulting in a small SIF emission. In the case of O_2-A, the dense vegetation (LAI $= 6$) produces a stronger multiple scattering inside the canopy, resulting in an increased reflected radiance, whereas SIF is only slightly increased. Aside from these physiological effects, it is necessary to consider the added effect of noise, which increases with radiance levels, and the atmospheric perturbation that cannot be perfectly compensated. These observed errors are in agreement with the work in [39].

Overall, the histograms of these error maps (see Fig. 9) indicate that the retrieval is performed with an accuracy below the mission requirements (red dashed line) for all the three main SIF products. The histograms show a multivalued error distribution due to the performance of the SIF retrieval in

the three vegetation classes. In addition, those pixels with an error above the mission requirements are mostly located in the following: 1) the vicinity of the clouds, due to scattering and stray-light contamination, and 2) the shaded regions, which can affect the atmospheric correction of those pixels.

V. Conclusions and Outlook

The selection of FLEX for ESA's future eighth Earth Explorer mission has been based on a competitive process for which the overall mission performance assessment relied on the results provided by FLEX-E.

In this paper, FLEX-E has been presented and applied for the evaluation of the mission performance and specifically to determine the accuracy of the retrieved Level-2 SIF products. This has been possible, on the one hand, due to the realism of the simulated environmental effects (e.g., natural variability of the key biophysical/atmospheric parameters, use of state-of-the-art RTMs, or consideration of bidirectional reflectance effects). On the other hand, the implemented instrumental and Level-1b calibration effects reproduced with great detail the actual instrument configuration. The results show that the Level-2 products are retrieved with an RRMSE below 4% for the integrated total SIF emission and an RMSE below 0.11 (0.09) $\mathrm{mW \cdot m^{-2} \cdot sr^{-1} \cdot nm^{-1}}$ for the SIF at the first (second) peak. Thereby, FLEX-E indicates the suitability of the proposed FLEX/S3 mission concept and implemented algorithms to retrieve SIF within the mission requirements. The validation of the results both at Level-1b and Level-2 demonstrates the suitability of the FLEX-E tool to perform tradeoff studies on the instrument design, reducing costs while keeping the SIF retrieval performance within the mission requirements. In addition, FLEX-E offers a framework that enables to test and optimize the retrieval algorithms, reducing the computation time and increasing the accuracy/precision of the retrieved products.

The design of FLEX-E is based on a generic E2ES architecture, which was adapted to reproduce the FLEX/S3 tandem mission. Its versatility allows the user to simulate a wide range of possible scenarios, from simple geometric patterns to complex scenes with realistic environmental conditions and sensor description. The main premise in the design and implementation of FLEX-E was its capability to reproduce the complexity of the FLEX mission, which is mainly driven by the geometric aspects of the tandem flight and the high spectral resolution of the FLORIS instrument. In addition, FLEX-E was conceived as a valuable tool to evaluate the performance of the final Level-2 mission products, which constrained the simulation of the reference scenarios. At the same time, FLEX-E was also designed with the purpose of being reused for the implementation of the FLEX ground processing and testing of Cal/Val procedures. While an overview of the architecture and implementation of the FLEX-E tool is here presented, it is expected that the proposed methodology will serve as a baseline for next-generation optical satellite mission simulators.

Future works will describe the implemented algorithms within the scene generator and Level-2 retrieval modules in greater detail.

References

[1] "Report for mission selection: FLEX," Eur. Space Agency, Noordwijk, The Netherlands, ESA SP-1330/2, 2 volume series, 2015.

[2] J. Moreno *et al.*, "FLEX/S3 tandem mission Performance Analysis and Requirements Consolidation Study (PARCS)," Univ. Valencia, Valencia, Spain, Tech. Rep. ESA Contract No. 4000105078/11/NL/AF, Study Final Rep., 2014. [Online]. Available: http://ipl.uv.es/flex-parcs/.

[3] G. Mohammed *et al.*, "FLEX/S3 tandem mission photosynthesis study," P&M Technol., Ste. Marie, ON, Canada, Tech. Rep. ESA Contract No 4000106396/12/NL/AF, Study Final Rep., 2014. [Online]. Available: http://www.flex-photosyn.ca/.

[4] C. de Negueruela *et al.*, "ARCHEO-E2E: A reference architecture for earth observation end-to-end mission performance simulators," in *Proc. SESP, Simul. EGSE facilities*, 2012, pp. 1–9 .

[5] ESA, "Open Simulation Framework (OpenSF) official webpage," accessed Jan. 21, 2016. [Online]. Available: http://eop-cfi.esa.int.

[6] J. P. Kerekes and D. A. Landgrebe, "Simulation of optical remote sensing systems," *IEEE Trans. Geosci. Remote Sens.*, vol. 27, no. 6, pp. 762–771, Nov. 1989.

[7] J. Kerekes and J. Baum, "Spectral imaging system analytical model for subpixel object detection," *IEEE Trans. Geosci. Remote Sens.*, vol. 40, no. 5, pp. 1088–1101, May 2002.

[8] A. Börner *et al.*, "SENSOR: A tool for the simulation of hyperspectral remote sensing systems," *ISPRS J. Photogramm. Remote Sens.*, vol. 55, no. 5/6, pp. 299–312, 2001.

[9] L. Guanter, K. Segl, and H. Kaufmann, "Simulation of optical remote-sensing scenes with application to the EnMAP hyperspectral mission," *IEEE Trans. Geosci. Remote Sens.*, vol. 47, no. 7, pp. 2340–2351, Jul. 2009.

[10] M. Scagliola *et al.*, "The CoReH2O end to end simulator: Architecture and simulation results analysis," in *Proc. IGARSS*, 2012, pp. 4541–4544.

[11] K. Segl *et al.*, "EeteS—The EnMAP end-to-end simulation tool," *IEEE J. Sel. Topics Appl. Earth Observations Remote Sens.*, vol. 5, no. 2, pp. 522–530, Apr. 2012.

[12] P. Lopez-Dekker *et al.*, "Biomass end-to-end mission performance assessment," in *Proc. IEEE IGARSS*, 2012, pp. 1602–1605.

[13] K. Segl, R. Richter, T. Küster, and H. Kaufmann, "End-to-end sensor simulation for spectral band selection and optimization with application to the Sentinel-2 mission," *Appl. Opt.*, vol. 51, no. 4, pp. 439–449, 2012.

[14] K. Segl, L. Guanter, and H. Kaufmann, "Simulation-based case studies for optimization of sensor design and image-based parameter retrieval using the EnMAP scene simulator," in *Proc. Hyperspectral Workshop*, 2010, pp. 1–4.

[15] M. Meroni *et al.*, "Performance of spectral fitting methods for vegetation fluorescence quantification," *Remote Sens. Environ.*, vol. 114, no. 2, pp. 363–374, 2010.

[16] A. Porcar-Castell *et al.*, "Linking chlorophyll a fluorescence to photosynthesis for remote sensing applications: Mechanisms and challenges," *J. Exp. Botany*, vol. 65, no. 15, pp. 4065–4095, Aug. 2014.

[17] F. Daumard *et al.*, "A field platform for continuous measurement of canopy fluorescence," *IEEE Trans. Geosci. Remote Sens.*, vol. 48, no. 9, pp. 3358–3368, Sep. 2010.

[18] C. Frankenberg *et al.*, "New global observations of the terrestrial carbon cycle from GOSAT: Patterns of plant fluorescence with gross primary productivity," *Geophys. Res. Lett.*, vol. 38, no. 17, Sep. 2011, Art. no. L17706.

[19] S. Kraft *et al.*, "FLORIS: Phase a status of the fluorescence imaging spectrometer of the earth explorer mission candidate FLEX," in *Proc. SPIE—Int. Soc. Opt. Eng.*, 2013, vol. 8889, pp. 1–12.

[20] C. Donlon *et al.*, "The Global Monitoring for Environment and Security (GMES) Sentinel-3 mission," *Remote Sens. Environ.*, vol. 120, pp. 37–57, 2012.

[21] "Sentinel-3 user handbook," Eur. Space Agency, Paris, France, ESA GMES-S3OP-EOPG-TN-13-0001, no. 1.0, Sep. 2013.

[22] "Earth observation CFI software official webpage," Eur. Space Agency, Paris, France, [accessed Apr. 27, 2015]. [Online]. Available: http://eop-cfi.esa.int/index.php/mission-cfi-software/eocfi-software.

[23] J. Rivera, N. Sabater, C. Tenjo, J. Vicent, and J. Moreno, "Synthetic scene simulator for hyperspectral spaceborne passive optical sensors: Application to ESA's FLEX/Sentinel-3 tandem mission," *Proc. 4th WHISPERS*, Lausanne, Switzerland, 2014.

[24] "CORINE land cover," Eur. Environ. Agency (EEA), Copenhagen, Denmark, EEA Rep., 1995, [accessed Apr. 27, 2015]. [Online]. Available: http://www.eea.europa.eu/publications/COR0-landcover.

[25] A. Inness *et al.*, "The MACC reanalysis: An 8 yr data set of atmospheric composition," *Atmos. Chem. Phys.*, vol. 13, no. 8, pp. 4073–4109, 2013.

[26] ASTER GDEM Validation Team, "ASTER global digital elevation model, version 2, summary of validation results," Ministry Econ., Trade Ind. (METI), Nat. Aeronaut. Space Admin. (NASA), Washington, D.C., USA, Tech. Rep., Aug. 2011.

[27] I. Reda and A. Andreas, "Solar position algorithm for solar radiation applications," Nat. Renew. Energy Lab. (NREL), Washington, DC, USA, Tech. Rep. NREL/TP-560-34302, 2003.
[28] C. Van Der Tol, W. Verhoef, J. Timmermans, A. Verhoef, and Z. Su, "An integrated model of soil-canopy spectral radiances, photosynthesis, fluorescence, temperature and energy balance," *Biogeosciences*, vol. 6, no. 12, pp. 3109–3129, 2009.
[29] A. Berk *et al.*, "MODTRAN™5: 2006 update," *Proc. SPIE*, 2006, vol. 6233, pp. 1–8.
[30] W. Verhoef and H. Bach, "Coupled soil-leaf-canopy and atmosphere radiative transfer modeling to simulate hyperspectral multi-angular surface reflectance and TOA radiance data," *Remote Sens. Environ.*, vol. 109, no. 2, pp. 166–182, Jul. 2007.
[31] L. Guanter, R. Richter, and H. Kaufmann, "On the application of the MODTRAN4 atmospheric radiative transfer code to optical remote sensing," *Int. J. Remote Sens.*, vol. 30, no. 6, pp. 1407–1424, 2009.
[32] R. Sundberg, S. Richtsmeier, and R. Harem, "Monte Carlo based hyperspectral scene simulation," in *Proc. 2nd WHISPERS*, 2010, pp. 1–4.
[33] U. Rascher *et al.*, "Sun-induced fluorescence—A new probe of photosynthesis: First maps from the imaging spectrometer HyPlant," *Global Change Biol.*, vol. 21, no. 12, pp. 4673–4684, 2015.
[34] D. Schläpfer, J. Nieke, and K. Itten, "Spatial PSF nonuniformity effects in airborne pushbroom imaging spectrometry data," *IEEE Trans. Geosci. Remote Sens.*, vol. 45, no. 2, pp. 458–468, Feb. 2007.
[35] L. Busetto, M. Meroni, G. Crosta, L. Guanter, and R. Colombo, "SpecCal: Novel software for in-field spectral characterization of high-resolution spectrometers," *Comput. Geosci.*, vol. 37, no. 10, pp. 1685–1691, 2011.
[36] J. Vicent *et al.*, "Propagation of spectral characterization errors of imaging spectrometers at level-1 and its correction within a level-2 recalibration scheme," in *Proc. SPIE—Int. Soc. Opt. Eng.*, 2015, vol. 9611, pp. 1–12.
[37] N. Sabater, J. Vicent, L. Alonso, J. Verreslst, and J. Moreno, "An atmospheric correction algorithm for FLEX/S3 tandem mission," in *Proc. 5th Int. Workshop Remote Sens. Vegetation Fluorescence*, 2014, pp. 1–6. [Online]. Available: http://www.congrexprojects.com/2014-events/14c04/proceedings.
[38] N. Sabater, J. Vicent, L. Alonso, J. Verreslst, and J. Moreno, "An atmospheric correction algorithm for FLuorescence EXplorer/Sentinel-3 tandem mission," in *Proc. 5th Int. Workshop Remote Sens. Vegetation Fluorescence*, 2016, pp. 1–6.
[39] S. Cogliati *et al.*, "Retrieval of sun-induced fluorescence using advanced spectral fitting methods," *Remote Sens. Environ.*, vol. 169, pp. 344–357, 2015.
[40] J. Verrelst, J. Rivera, L. Alonso, R. Lindstrot, and J. Moreno, "Potential retrieval of biophysical parameters from FLORIS, S3-OLCI and its synergy," in *Proc. IEEE IGARSS*, 2012, pp. 7121–7124.
[41] FLEX MAG and M. Drusch, "FLEX Mission Requirements Document (MRD)," Eur. Space Agency (ESA), Paris, France, Tech. Rep. v1.0, May 2011.

Jorge Vicent received the B.Sc. degree in physics from the University of Valencia, Valencia, Spain, in 2008 and the M.Sc. degree in physics from the EPFL, Lausanne, Switzerland, in 2010.

Since August 2011, he has been with the Laboratory of Earth Observation at the Image Processing Laboratory, University of Valencia, as a Research Assistant and Ph.D. candidate. He is currently involved in the preparatory activities of the Fluorescence Explorer. His research interests include the modelling of Earth Observation satellites, system engineering, radiative transfer modelling, atmospheric correction, and hyperspectral data analysis.

Neus Sabater received the B.Sc. degree in physics and the M.Sc. degree in remote sensing from Universitat de Valencia, Valencia, Spain, in 2010 and 2013, respectively. She also received the award of the University of Valencia, for the best student records in the M.Sc. of remote sensing (2012–2013).

Since August 2012, she has been involved in the activities of the Laboratory for Earth Observation at the Image Processing Laboratory, University of Valencia, as a Research Technician. Main activities during this period were related to the development of the preparatory activities of the Fluorescence Explorer mission. In 2013, she was awarded a Ph.D. scholarship from the Spanish Ministry of Economy and Competitiveness, associated to the Ingenio/Seosat Spanish space mission. Her main research and personal interests include atmospheric correction, atmospheric radiative transfer, meteorology, and hyperspectral remote sensing.

Carolina Tenjo received the B.Sc. degree in geology from Universidad Nacional de Colombia, Bogotá, Columbia, in 2004 and the M.Sc. degree in remote sensing from Universitat de Valencia, Valencia, Spain, in 2013, where she has been working toward the Ph.D. degree in remote sensing since 2012. She is currently with the University of Valencia.

She is currently involved in the European Space Agency's Fluorescence Explorer research activities. Her research interest includes the development of algorithms for remote sensing applications in water quality and software development applied to remote sensing.

Juan Ramón Acarreta received the M.Sc. degree in 1994 from the Universidad Complutense, Madrid, Spain, with work regarding photometry on middle-active galaxies, and the Ph.D. degree in 1999 fom the Universidad Autonoma, Madrid, on radiative transfer modelling to analyze the atmospheres of the Giant Planets.

During the years 2000–2004 he held a postdoctoral position at the Koninklijk Nederlands Meteorologisch Instituut, Holland, on subjects related with O2-O2 cloud pressure retrieval (OMI), thermodynamic phase retrieval (SCIAMACHY), and optical cross-calibration analysis. Since the year 2005, he has been working on Deimos-Space on areas related with E2E simulators and L0/L1 processing. The projects, being under the scope of ESA/EUMETSAT activities, refer to missions like GOCE, EARTHCARE, COREH2O, SENTINEL3, CARBONSAT, FLEX, and METEOSAT-SG, either at Prime or subcontractor level. Specifically, his duties are processor development, integration, and verification combined with managerial activities.

María Manzano received the M.Sc. degree in mathematics from the Complutense University of Madrid, Madrid, Spain.

With 14 years of experience in GMV, she has been involved in projects related to end-to-end simulators for Earth Observation missions (PREMIER-E2ES and FLEX-E), mainly in tasks related to the simulator architecture and interface definition, and the implementation of the performance evaluation module. She has also large experience in GNSS-related projects, including GNSS receiver simulators and signal characterization for ground and spatial applications.

Juan Pablo Rivera received the B.Sc. degree in agricultural engineering from the National University of Colombia, Bogotá, Columbia, and the University of Valle, Cali, Colombia, in 2001, the Master's degree in irrigation engineering from the Centro de Estudios y Experimentación de Obras Publicas (CEDEX), El Goloso, Spain, in 2003, and the M.Sc. and Ph.D. degrees in remote sensing from the University of Valencia, Valencia, Spain.

Since January 2011, he has been a member of the Laboratory for Earth Observation, Image Processing Laboratory, University of Valencia. He is currently involved in the preparatory activities of the European Space Agency's Fluorescence Explorer mission. His research interests include the retrieval of vegetation properties using airborne and satellite data, leaf and canopy radiative transfer modeling, and hyperspectral data analysis.

Pedro Jurado received the M.Sc. degree in aerospace engineering from the Politecnica de Madrid University, in 2004, the MBA from the UNED University, Spain, in 2014, and the Optical Instrument Design professional certificate from UC Irvine, Irvine, CA, USA, in 2015.

Since May 2008, he has been working as a contractor on Future Missions for Earth Observation in the European Space Agency/European Space Research and Technology Centre (ESTEC) as a Future Mission System Engineer. He is currently involved in the preparatory activities of the Fluorescence Explorer as Mission Performance and System Operation Engineer.

Raffaella Franco received the diploma degree in physics from the University of Torino, Torino, Italy, in 1984.

She worked in Aeritalia, now Thales Alenia Space, where she was responsible for the onboard SW of the Tethered Satellite System. She joined the European Space Agency (ESA) in 1988 as Attitude and Orbit Control Analyst to support, among others, Olympus, Soho, and Envisat projects. In 1995, she moved to system engineering, defining R&D activities for satellite systems verification and validation by simulation and applying them to ATV, Smart-1, Proba-1&3, and EGNOS. In 2001, she joined the Galileo project where she was responsible for the overall coordination of system verification activities and tools, particularly the Galileo end-to-end simulation facility. Since 2005, she started promoting the end-to-end performance assessment concept for Earth Observation missions by defining methods and tools which are now applied to Earth Explorer and Sentinel missions. Following her involvement in EarthCARE E2ES, she has been responsible for the BIOMASS and Fluorescence Explorer end-to-end mission performance simulators.

Her current activities include E2E scientific performance assessment for ESA science missions (pilot projects for Euclid and SSA-NEO) and Sentinel-3 CalVal planning and coordination.

Luis Alonso received the B.Sc. degree in physics and the M.S. degree in environmental physics from the University of Valencia, Valencia, Spain, in 1999 and 2002, respectively, while working on the geometric correction of airborne and spaceborne remote sensing imagery.

He is member of the Laboratory for Earth Observation at the Image Processing Laboratory of the University of Valencia, where he studies the remote sensing of chlorophyll fluorescence at canopy level. He has participated in several preparatory studies for the Fluorescence Explorer candidate mission for the European Space Agency's Earth Explorers as well as for Copernicus Sentinel-2 and Sentinel-3.

Jochem Verrelst received the M.Sc. degrees in tropical land use and in geoinformation science both in 2005 and the Ph.D. degree in remote sensing in 2010 from Wageningen University, Wageningen, The Netherlands. His dissertation focused on the spaceborne spectrodirectional estimation of forest properties.

Since March 2010, he has been a Marie Curie Postdoctoral Fellow at the Laboratory for Earth Observation, Image Processing Laboratory, University of Valencia, Valencia, Spain. He is currently involved in preparatory activities of the Fluorescence Explorer. His research interests include the retrieval of vegetation properties using airborne and satellite data, canopy radiative transfer modeling, and multiangular and hyperspectral data analysis.

José Moreno (A'89–M'09) received the M.Sc. degree in physics in 1986 and the Ph.D. degree in theoretical physics, both from the University of Valencia, Valencia, Spain, in 1992.

He is currently a Professor with the Department of Earth Physics and Thermodynamics, Faculty of Physics, University of Valencia, teaching and working on different projects related to remote sensing and space research and Director of the Laboratory for Earth Observation (LEO) Image Processing Laboratory/Scientific Park. His main work is related to the modelling and monitoring of land surface processes by using remote sensing techniques. He has been involved in many international projects and research networks, as well as in preparatory activities and exploitation programs of several satellite missions (ENVISAT, CHRIS/PROBA, GMES/Sentinels-1/-2/-3, and SEOSAT). He is currently Principal Investigator and Chairman of the Mission Advisory Group for the Fluorescence Explorer (FLEX), an Earth Explorer Mission of the European Space Agency (ESA).

Dr. Moreno has served as Associate Editor for the IEEE TRANSACTIONS ON GEOSCIENCE AND REMOTE SENSING (1994–2000) and has been a member of the ESA Earth Sciences Advisory Committee, the Space Station Users Panel, and other international advisory committees.